Temperature-Stable Silicon Oxide (SilOx) Micromechanical Resonators

R. Tabrizian, G. Casinovi and F. Ayazi

IEEE Transactions on Electron Devices
vol. 60, no. 8, pp. 2656–2663, August 2013

Abstract

This paper presents a passive temperature compensation technique that can provide full cancellation of the linear temperature coefficient of frequency (TCF_1) in silicon resonators. A uniformly distributed matrix of silicon dioxide pillars is embedded inside the silicon substrate to form a homogenous composite silicon oxide platform (SilOx) with nearly perfect temperature-compensated stiffness moduli. This composite platform enables the implementation of temperature-stable microresonators operating in any desired in- and out-of-plane resonance modes. Full compensation of TCF_1 is achieved for extensional and shear modes of SilOx resonators resulting in a quadratic temperature characteristic with an overall frequency drift as low as 83 ppm over the industrial temperature range (−40 °C to 80 °C). Besides a 40 times reduction in temperature-induced frequency drift in this range, SilOx resonators exhibit improved temperature stability of *Q* compared with their single crystal silicon counterparts.

Copyright Notice

Temperature-Stable Silicon Oxide (SilOx) Micromechanical Resonators

Roozbeh Tabrizian, *Student Member, IEEE*, Giorgio Casinovi, *Senior Member, IEEE*, and Farrokh Ayazi, *Fellow, IEEE*

***Abstract*— This paper presents a passive temperature compensation technique that can provide full cancellation of the linear temperature coefficient of frequency (TCF_1) in silicon resonators. A uniformly distributed matrix of silicon dioxide pillars is embedded inside the silicon substrate to form a homogenous composite silicon oxide platform (SilOx) with nearly perfect temperature-compensated stiffness moduli. This composite platform enables the implementation of temperature-stable microresonators operating in any desired in- and out-of-plane resonance modes. Full compensation of TCF_1 is achieved for extensional and shear modes of SilOx resonators resulting in a quadratic temperature characteristic with an overall frequency drift as low as 83 ppm over the industrial temperature range (−40 °C to 80 °C). Besides a 40 times reduction in temperature-induced frequency drift in this range, SilOx resonators exhibit improved temperature stability of Q compared with their single crystal silicon counterparts.**

***Index Terms*— High quality factor, homogenous composite, low insertion loss, silicon dioxide pillar matrix, silicon oxide (SilOx), temperature coefficient of frequency (TCF), temperature compensated crystal oscillator (TCXO), temperature compensation.**

I. Introduction

SILICON resonators have gained an increasing interest for timing and frequency reference applications [1]. The ability to offer low impedances at high frequencies and the high intrinsic quality factor (Q) of silicon [2] makes such resonators very attractive for low phase noise high frequency reference oscillators. However, the main drawback of silicon resonators is their relatively high temperature coefficient of frequency (TCF), which results in a large temperature-induced frequency drift. Various active [3]–[7] and passive [8]–[16] temperature compensation techniques were proposed for microelectromechanical (MEMS) resonators. Although active compensation techniques provide real-time frequency control with high precision, they increase power consumption and introduce undesired noise and complexity into the system. On the other hand, full or partial compensation of the large linear TCF of silicon resonators by means of conventional passive techniques was only achieved in thin flexural and extensional resonators [8], [9] and specific bulk acoustic wave resonance modes in certain crystallographic orientations [10], [16].

In this paper, we present a novel passive temperature compensation technique that can realize silicon-based composite platforms with temperature-compensated acoustic properties, for implementation of temperature-stable devices oriented in arbitrary crystallographic directions, and operating in any in- and out-of-plane resonance modes. Using this technique, full compensation of the large linear TCF is achieved simultaneously for several resonance modes of microresonators without degradation of other important performance metrics such as Q and insertion loss (IL).

II. SiO_2 Temperature Compensation in Resonators

The temperature sensitivity of the resonance frequency (f_{res}) of a resonator can be defined using its temperature coefficients:

$$f_{\text{res}}(T) = f_0 \cdot \sum_{n=0}^{\infty} \text{TCF}_n \cdot (T - T_0)^n \tag{1}$$

where f_0 is the resonance frequency at an arbitrary operating temperature T_0, and TCF_n is the nth order TCF.

$$\text{TCF}_n = \frac{1}{n! f_0} \cdot \frac{\partial^n f_T}{\partial T^n}|_{T=T_0}. \tag{2}$$

The finite TCF_i of the resonance modes excited in a micromechanical resonator is a result of temperature sensitivity of the resonator dimensions as well as of several material properties such as its elastic moduli (λ), Poisson's ratio (υ), and mass density (ρ). For the case of in-plane bulk acoustic resonance modes of an infinitely long ($L \to \infty$) and thin/thick ($H \to 0$ or ∞) acoustic waveguide of width W, the resonance frequency of the nth width extensional (WE) and width shear (WS) bulk modes are given by

$$f_{\text{res}} = \frac{n}{2W}\sqrt{\lambda/\rho} \tag{3}$$

where λ is the effective elastic modulus—either Young's (E) or shear modulus (G)—of the resonator material in the wave propagation direction. It follows from (3) that for the bulk acoustic modes, TCF_i is related to the intrinsic material properties by

$$f_{\text{res}} = \frac{1}{2}(TC\lambda_i + \text{CTE}_i) \tag{4}$$

where $\text{TC}\boldsymbol{\lambda}_i (= 1/i!\lambda_0 \cdot (\partial^i \lambda_T)/(\partial T^i|_{T=T_0}))$ is the temperature coefficient of the elastic modulus and

Manuscript received March 9, 2013; revised May 30, 2013; accepted June 14, 2013. Date of publication July 9, 2013; date of current version July 19, 2013. This work was supported in part by Integrated Device Technology Inc. and the National Science Foundation EAGER under Grant 1057320. The review of this paper was arranged by Editor A. M. Ionescu.

The authors are with the School of Electrical and Computer Engineering, Georgia Institute of Technology, Atlanta, GA 30332 USA (e-mail: roozbeh@gatech.edu; giorgio.casinovi@ece.gatech.edu; ayazi@gatech.edu).

Color versions of one or more of the figures in this paper are available online at http://ieeexplore.ieee.org.

Digital Object Identifier 10.1109/TED.2013.2270434

$\mathrm{CTE}_i (= 1/i!W_0 \cdot (\partial^i W_T)/(\partial T^i|_{T=T_0}))$ is the coefficient of thermal expansion of the material.

Unlike quartz crystal resonators [17], the temperature-induced frequency drift of the MEMS resonators is mainly determined by their linear temperature coefficient ($\mathrm{TCF}_1 = (TC\lambda_1 + \mathrm{CTE}_1)/2$) over the temperature range of interest. In native single crystal silicon (SCS), $\mathrm{TC}\boldsymbol{\lambda}_1$ ranges between -47 and -63 ppm/°C depending on the resonance particle polarization and mode of operation (shear or extensional). This variation is a result of dissimilar temperature characteristics of different stiffness coefficients of silicon. Considering the relatively small CTE_1 of silicon (~2.6 ppm/°C), the large value of $\mathrm{TC}\boldsymbol{\lambda}_1$ is mainly responsible for the TCF_1 of silicon bulk acoustic resonators, which typically ranges between -22 and -30 ppm/°C.

Although the TCF of bulk acoustic modes in infinitely long and thin waveguides can be related to the intrinsic material properties through (4), a similarly simple relationship does not exist for all the resonance modes excited in micromechanical structures with finite dimensions. This is due to the fact that the resonance frequency of these modes cannot be related to the material properties and resonators dimensions through a simple closed-form expression; and unlike bulk modes, all different independent elastic constants (E, G, and υ) may contribute effectively in defining the resonance frequency. Hence, a passive compensation technique should provide full temperature compensation for all independent elastic constants to be effective for all resonance modes. In micromechanical resonators implemented in native SCS, the large negative $\mathrm{TC}\boldsymbol{\lambda}_1$ can be compensated by the addition of a material with positive $\mathrm{TC}\boldsymbol{\lambda}_1$ such as silicon dioxide (SiO_2), thus forming a composite Si/SiO_2 structure. The degree of temperature compensation of $\mathrm{TC}\boldsymbol{\lambda}_1$ depends on both the amount and the configuration of SiO_2 distribution relative to Si in the composite structure.

A. Surface Oxide Compensation

The compensating SiO_2 can be added in the form of layers covering the surfaces of a silicon resonator; we refer to this method as surface oxide compensation. In this case, the resonant structure is composed of several layers of different materials stacked in certain directions. They include one or more compensation layers and possibly a piezoelectric electromechanical transducer sandwiched between metallic electrodes [aluminum nitride (AlN) and molybdenum (Mo) layers in Fig. 1(a)]. The overall TCF_1 of such a composite resonator with surface SiO_2 compensation operating in WE or WS bulk acoustic modes can be estimated as follows:

$$\mathrm{TCF}_1 \approx \frac{1}{2}\sum_i \frac{T_i}{T_{\mathrm{res}}}(TC\lambda_{1,i} + \mathrm{CTE}_{1,i}) \tag{5}$$

where $\mathrm{TC}\boldsymbol{\lambda}_{1,i}$, $\mathrm{CTE}_{1,i}$, and T_i are the temperature coefficient of the elastic modulus, the linear coefficient of thermal expansion, and the thickness of the ith layer, respectively, and T_{res} is the overall thickness of the stack. Since the SiO_2 layer is placed in parallel with a silicon layer with a much larger elastic modulus, it follows from (5) that surface SiO_2 compensation becomes less efficient as the relative thickness of silicon in the stack increases. Furthermore, since this technique provides only one degree of freedom, i.e., the thickness of the SiO_2 layer, the compensation effect on various elastic constants and hence different resonance modes differs considerably.

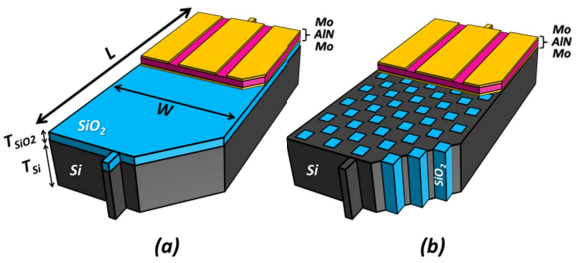

Fig. 1. Silicon resonators with piezoelectric transduction (a) with surface oxide compensation and (b) with bulk oxide compensation.

B. Bulk Oxide Compensation

To increase the relative contribution of SiO_2 in $\mathrm{TC}\boldsymbol{\lambda}_1$ of a composite Si/SiO_2 structure, the compensating SiO_2 can be embedded in the bulk of the silicon resonant structure: this is referred to as bulk oxide compensation. In this technique, a matrix of SiO_2 pillars with a desirable pattern is distributed inside the body of a silicon resonator to form a silicon oxide (SilOx) composite resonator [18]. In this manner, since the additional SiO_2 can be embedded in series with silicon in the path of in-plane propagating acoustic waves, full compensation of the large TCF_1 for different resonance modes can be achieved by adding a minimum amount of SiO_2. This makes bulk compensation fully compatible with the limitations of standard microfabrication processes.

Furthermore, this technique is scalable with resonator thickness and can be applied even to thick resonant structures. Last, but not least, the in-plane lateral dimensions of the SiO_2 pillars as well as the pattern and density of their distribution in the matrix can be exploited as additional degrees of freedom to simultaneously compensate multiple resonance modes through the compensation of corresponding elastic constants in desired orientation.

III. Resonator Design

A. SilOx Platforms With Bulk Oxide Compensation

In micromechanical resonators, each resonance mode can be interpreted as a superposition/interaction of longitudinal and shear quasi-plane waves propagating in arbitrary directions and reflecting back from the stress-free boundaries of the structure. Therefore, the distribution of the SiO_2 pillars in the Si substrate should be designed so as to: 1) facilitate the propagation of the acoustic waves corresponding to the desired modes of operation without destructive dispersion and 2) provide adequate distribution in regions with high acoustic energy density.

Thus, to provide temperature compensation for desirably all resonance modes, a proper matrix of pillars should be as uniform as possible, forming a nearly homogenous SilOx composite structure with temperature-compensated elastic moduli. Such a homogenous platform is called a SilOx matrix hereafter. A rectangular SilOx resonator oriented in ⟨110⟩

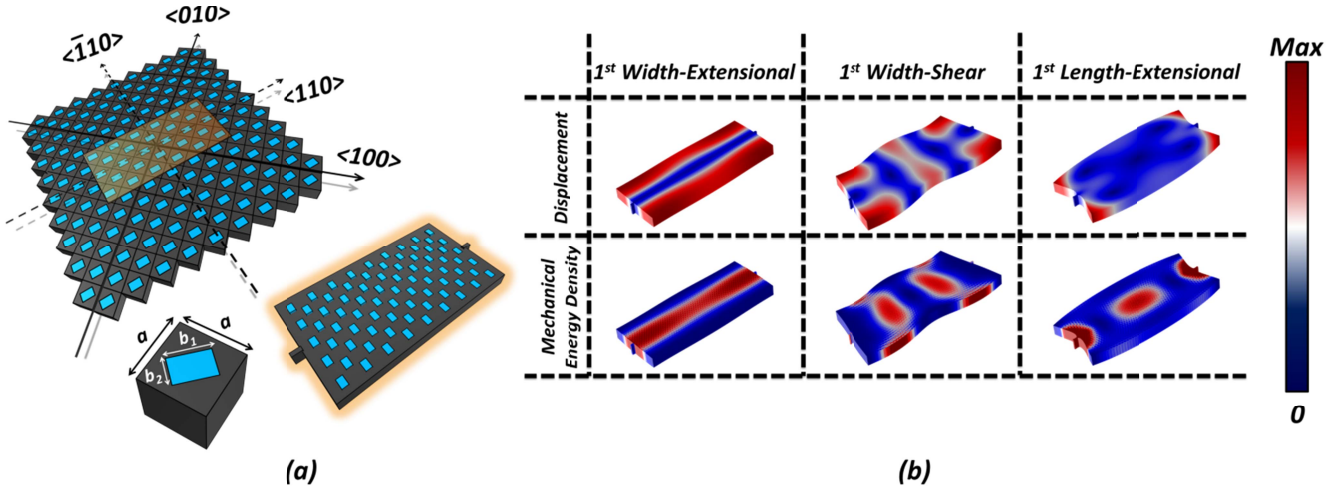

Fig. 2. (a) Rectangular SilOx resonator. a and $b_{1,2}$ are SilOx unit and SiO_2 pillar lateral dimensions, respectively. (b) Displacement and mechanical energy density of a rectangular SilOx resonator for its WE_1, WS_1, and LE_1 modes.

crystalline direction of silicon is shown in Fig. 2(a). The displacement and mechanical energy density fields for WE_1, WS_1, and length-extensional (LE_1) modes of the rectangular parallelepiped SilOx structure of Fig. 2(a) are shown in Fig. 2(b). Considering the uniform distribution of SiO_2 pillars, the composite resonator shown in Fig. 2 can be regarded as an array of SilOx units [Fig. 2(a)]. For the purpose of approximate analytical modeling, these units can be replaced by an equivalent cell with similar dimensions but made of a homogeneous material. Then, the equivalent elastic modulus (λ_{SilOx}) and mass density (ρ_{SilOx}) can be estimated as a function of R_1, the volumetric ratio of SiO_2 in the SilOx unit cell with square cross-section ($R_1 = V_{Sio_2}/V_{cell} = b_1 \cdot b_2/a^2$) and R_2, the in-plane aspect ratio of SiO_2 pillars ($R_2 = b_1/b_2$). Using these equivalent values in (4), R_1 and R_2 can be calculated to achieve full compensation of $TC\lambda_1$ ($\lambda = E$ and G) for the composite SilOx platform in desired crystalline orientation of silicon. These approximate values of R_1 and R_2 are then taken as the starting point for ANSYS numerical simulations which are used to refine first cut designs derived from the analytical model. Lateral (in-plane) SiO_2 pillars dimensions as well as their distribution density in silicon substrate are optimized to minimize the overall frequency drift for different modes of extensional and shear types [Fig. 2(b)], over the temperature range of interest. Only a few iterations of this procedure are needed to generate resonator designs that minimized the resonance frequency drift over the temperature range of interest. The simulated temperature characteristic of the WE_1 and WS_1 modes for a temperature-compensated SilOx resonator is shown in Fig. 3. Full cancellation of TCF_1 results in a quadratic temperature characteristic of the resonance frequency. Therefore, the overall frequency drift over the temperature range of interest can be minimized by locating the temperature characteristic turnover point at the center of the temperature range of interest (20 °C).

IV. Fabrication

The SiO_2 pillar matrix is formed by etching square-shaped trenches inside the device layer of a silicon-on-insulator wafer.

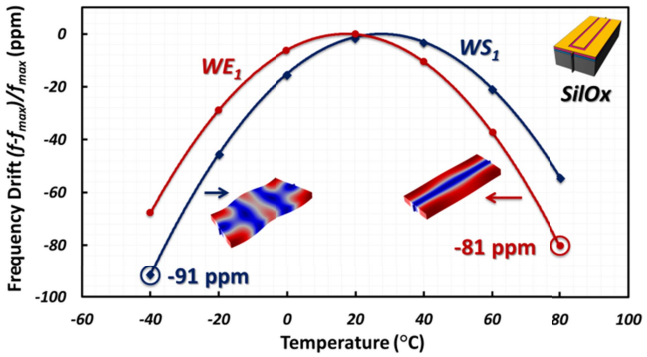

Fig. 3. Simulated temperature characteristic of a TCF_1 compensated SilOx resonator operating in WE_1 and WS_1 modes.

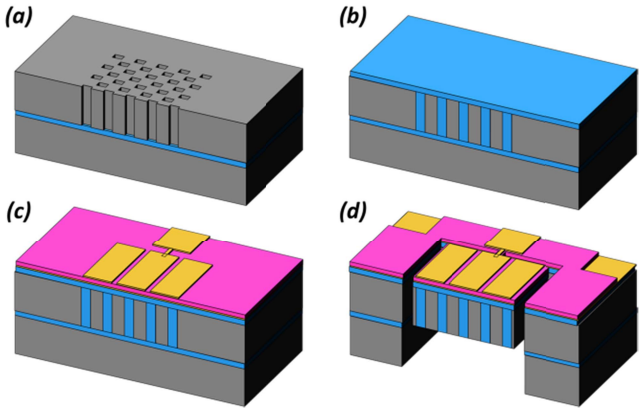

Fig. 4. Summarized fabrication process flow of the SilOx resonator.

These trenches are then filled by multiple deposition and etching steps of low-pressure chemical vapor deposition SiO_2. An additional thin layer of SiO_2 is left on the surface of the SilOx structure to provide smooth surfaces required for the deposition of a high-quality AlN film. The rest of the process is similar to the one described in [12] and is summarized in Fig. 4.

The SEM images of a fabricated SilOx resonator with AlN piezoelectric signal transduction are shown in Fig. 5. The SiO_2

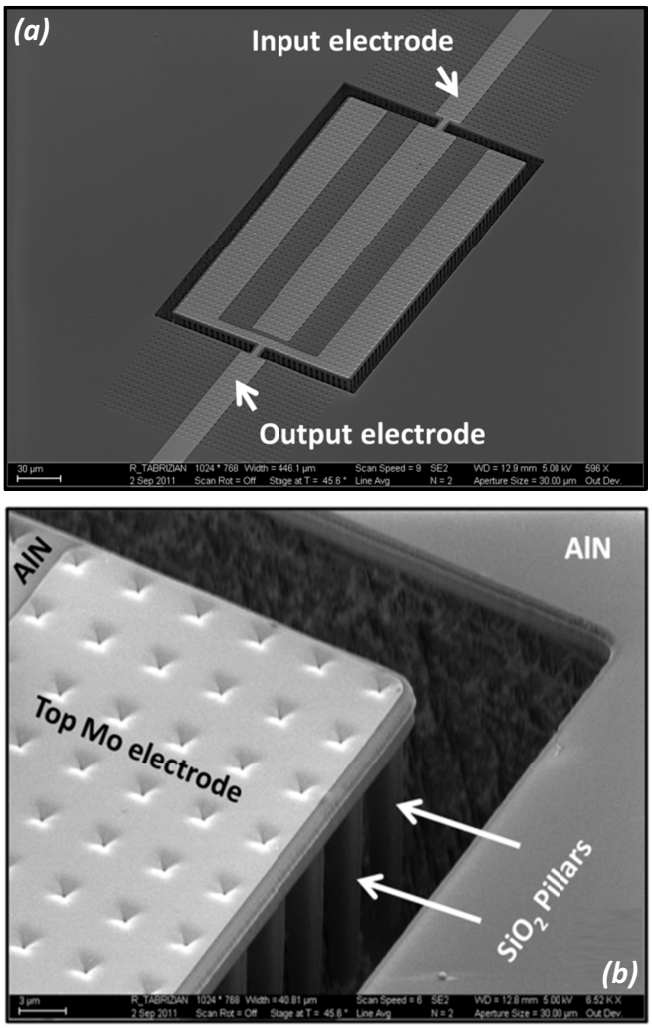

Fig. 5. (a) Temperature-stable AlN-on-SilOx resonator. (b) SiO_2 pillars extruding from the resonator sidewall.

pillars are made visible by purposely over-etching the silicon body of the resonator from a backside release opening.

V. Measurement

Any SilOx resonator may possess multiple resonance modes in the vicinity of the desired temperature-compensated modes, some of which may be under-/over-compensated over the temperature range of interest or have a turnover point of temperature characteristic in undesirably lower high temperatures. In frequency reference applications [19], the oscillator may lock into any of the excited modes in the operation band of the trans-impedance amplifier. Therefore, proper design of the electromechanical transducer is essential to excite the resonance modes of interest, while suppressing undesired spurious modes situated in a relatively wide frequency span around it. In this paper, AlN piezoelectric transduction is used since mode selection and suppression can be easily done by proper patterning of the metallic electrodes. Furthermore, since this transduction scheme does not require a dc polarization voltage for operation, it is intrinsically immune to dielectric charging effect which may induce

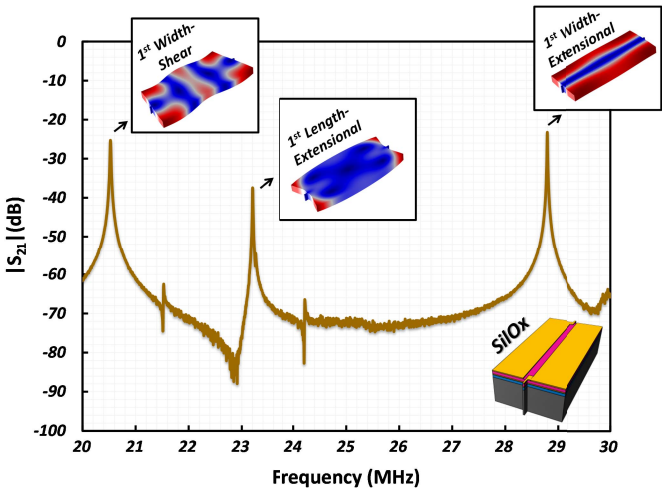

Fig. 6. Large-span frequency response of a SilOx resonator with proper electrode configuration to excite three modes in the measured span.

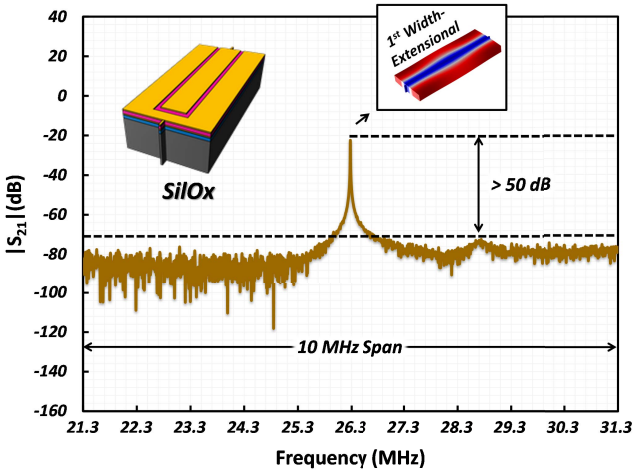

Fig. 7. Frequency response of a SilOx resonator with proper AlN transducer designed for effective excitation of WE_1 mode, resulting in a spurious-free 10-MHz span around the temperature-compensated resonance mode.

frequency fluctuations over time in capacitive resonators with surface SiO_2 compensation [20].

The frequency response of a rectangular SilOx resonator with an electrode design resulting in excitation of all first WE and LE, as well as WS modes, in a 10-MHz frequency span is shown in Fig. 6.

The frequency response of a 26.3-MHz SilOx resonator with proper electrode configuration for excitation of the first WE mode in a spurious-free 10-MHz span [Fig. 5(a)] is shown in Fig. 7. The IL of the WE_1 resonance mode is >50 dB higher than the noise floor, thus facilitating the implementation of MEMS oscillators [19] without any concern about locking to an undesired mode.

A. Resonator Performance Characterization

Two-port SilOx resonators are tested in a temperature-controlled environmental chamber. A vector network analyzer in two-port configuration is used to measure the

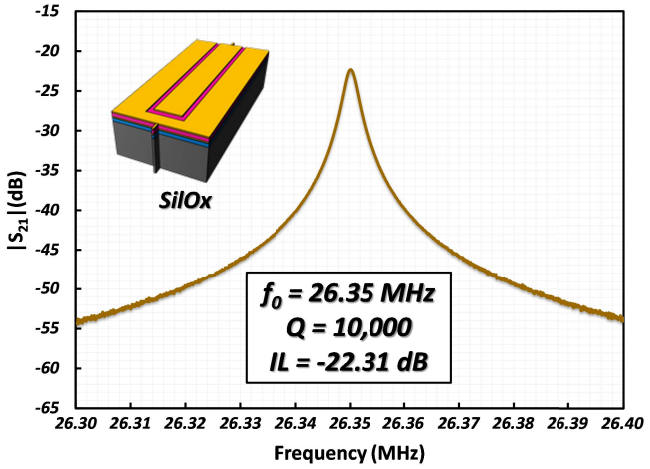

Fig. 8. Frequency response of the SilOx resonator in a 100-kHz frequency span around its WE_1 resonance mode, measured in air.

frequency response of the devices as well as their temperature characteristics.

The frequency response of the SilOx resonator in a 100-kHz frequency span around the WE_1 resonance mode is shown in Fig. 8. A high Q of ~10 000 is measured at 26.3 MHz in air with an IL of −22.35 dB.

B. Temperature Characterization

The temperature characteristics of the SilOx resonators are measured over the range of −40 °C to 80 °C and compared with their SCS counterparts implemented in the same batch. The temperature characteristic of the resonance frequency for WE_1, WS_1, and LE_1 modes of SCS and SilOx resonators with similar dimensions and electrode configuration is shown in Fig. 9.

The difference between TCF_1 of different modes in the SCS device is due to the difference in the temperature coefficients of the stiffness constants of silicon [21]. In the case of SilOx resonator, the TCF_1 compensation is achieved for several in-plane resonance modes of a single device. Frequency drifts as small as 83 ppm are measured for WE_1 mode over the entire temperature range of −40 °C to 80 °C. This corresponds to a 40 times improvement in the overall frequency drift compared with a noncompensated silicon resonator. Furthermore, the quadratic temperature characteristic achieved by cancellation of TCF_1 possesses a turnover point between 20 °C and 25 °C with a zero TCF_1. This is very close to the turnover point of the simulated temperature characteristic (20 °C), which guarantees the minimum overall frequency drift over the temperature range of −40 °C to 80 °C.

However, higher turnover temperatures may be required for oven-controlled crystal oscillator applications since they need to operate at a constant temperature exceeding the operational temperature range of interest (typically 90 °C). This can be achieved lithographically by a slight modification of the volumetric ratio of oxide in SilOx unit (R_1) to locate the turnover point at a higher temperature [Fig. 10].

SilOx temperature-compensated resonators exhibit robust Q over the entire temperature range. Fig. 11 compares the

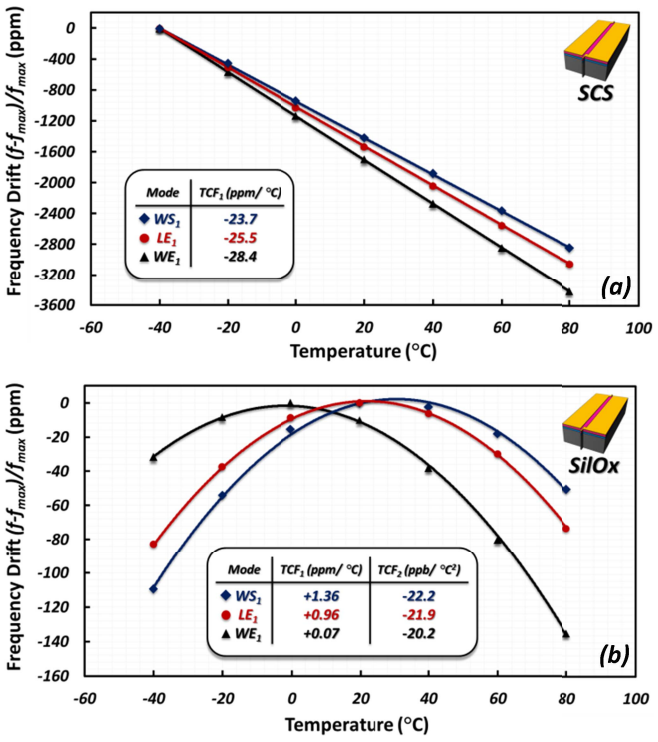

Fig. 9. Measured temperature characteristic of the resonance frequency of three different resonance modes of (a) SCS and (b) SilOx resonators. The electrode configuration used for excitation of all modes is shown as well.

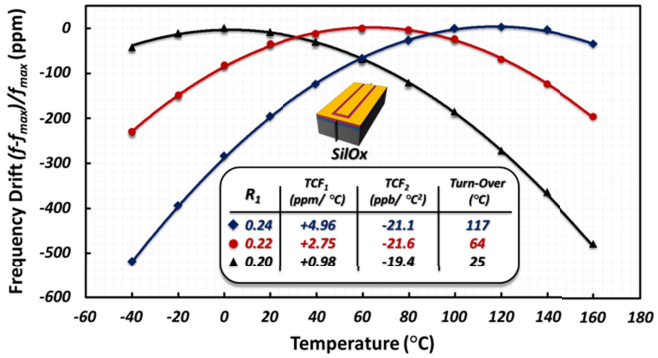

Fig. 10. Measured temperature characteristic of the WE_1 resonance frequency for three SilOx resonators with different volumetric ratio of SiO_2 in SilOx unit (R_1). Turnover temperature tailoring is realized by slight modification of R_1.

Q temperature characteristic of the SilOx resonator of Fig. 8 with its SCS counterpart with similar dimension and transducer configuration.

Besides providing high performance temperature-compensated in-plane WE, LE, and WS modes, SilOx platforms can be optimized to provide temperature-compensated thickness modes with high quality factors. The large-span frequency response of a rectangular SilOx resonator is shown in Fig. 12. The resonance frequencies and measured Q values of three in- and out-of-plane extensional modes are shown in [Fig. 12(a)], while their temperature characteristics of resonance frequency are compared in [Fig. 12(b)].

Unlike in-plane extensional and shear modes, where the resonance frequency can be defined lithographically

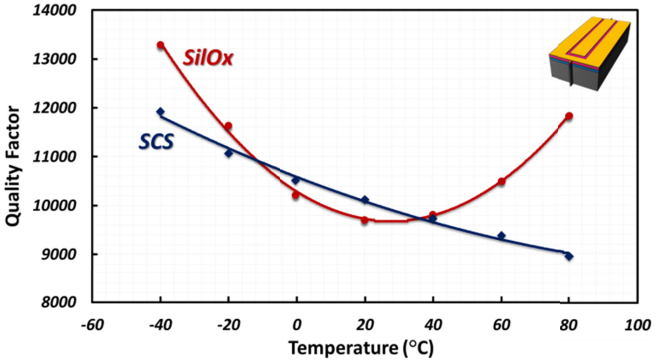

Fig. 11. Temperature characteristic of the Q for SCS and SilOx resonators with similar dimensions and transducer configuration, operating in WE_1 mode.

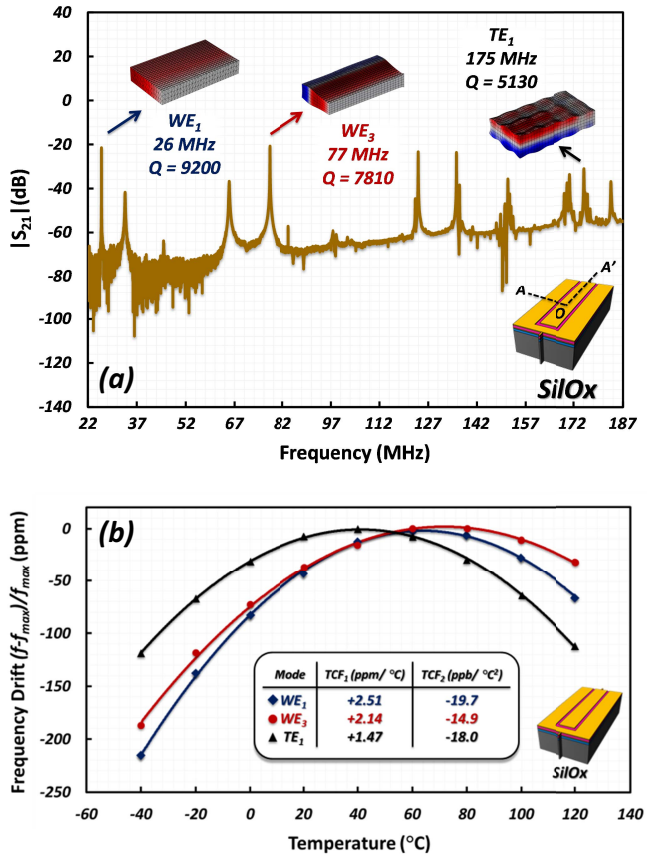

Fig. 12. (a) Large-span frequency response of a rectangular SilOx resonator. (b) Temperature characteristic of resonance frequency for $WE_{1,3}$ and TE_1 modes.

and is independent of resonator thickness, the resonance frequency of the thickness-extensional (TE) mode is mainly defined by the thickness of the structure as well as the distribution density of SiO_2 pillars. Hence, by selecting appropriate thicknesses, SilOx resonators can be implemented to provide two high-Q temperature-compensated modes with independent resonance frequencies and orthogonal particle displacement. This can potentially cut the manufacturing cost of MEMS temperature-stable oscillators into half, since a single device can be used as a frequency reference at two substantially different and independent frequencies.

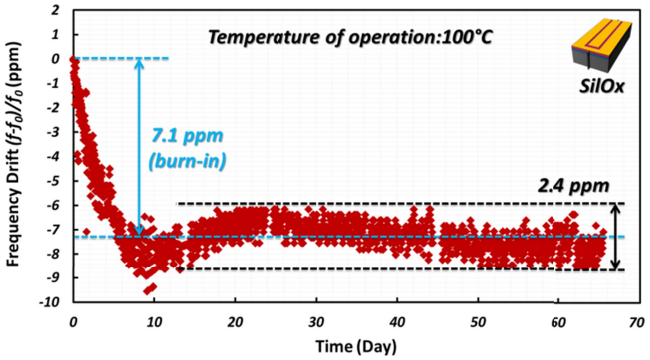

Fig. 13. Long-term stability of the resonance frequency for a temperature-stable SilOx resonator operating in WE_1 mode at 100 °C; burn-in period as well as stabilized range of operation are indicated.

C. Stability

To measure the resonance frequency stability of SilOx resonators, a number of devices are mounted on boards using a small piece of copper tape and wire bonded to subminiature (SMA) connector pads. Both long-term stability and short-term hysteresis measurements are performed by placing the mounted test boards under a ∼100-μtorr vacuum inside a temperature-controlled environmental chamber. This is done to eliminate any possible environmental source of frequency and Q perturbation. The temperature accuracy of the environmental chamber is ±1 °C.

The long-term stability of the resonance frequency for a temperature-stable SilOx resonator is shown in Fig. 13. An elevated temperature of 100 °C is used to accelerate aging processes requiring thermal activation energy.

A burn-in drift of 7.1 ppm over a period of ∼10 days is observed in these resonators prior to frequency stabilization. This burn-in drift is comparable with that of quartz crystal resonators [22] and can be attributed to the large effective surface between Si and SiO_2 in SilOx resonators, which can aggravate the stress induced due to CTE mismatch at the interface of SiO_2 pillars and SCS. After the burn-in period, a frequency fluctuation of ±1.2 ppm is observed. Considering the local TCF_1 of −3 ppm/°C at 100 °C (i.e. $1/f_0 \cdot \partial f_0/\partial T|_{T=100°C} = -3\,\text{ppm/°C}$) for the SilOx resonator beside temperature accuracy of the measurement unit, this variation can be attributed to temperature instabilities of environmental chamber and the resolution of temperature sensor.

Besides long-term stability, short-term hysteresis measurement is also performed on SilOx resonators to study the effect of rapid environmental temperature changes. Since SilOx composite resonators with AlN signal transduction are composed of different materials with various CTEs, rapid temperature variations may induce axial stresses, resulting in frequency drifts or even cracks in the device [23].

Hysteresis characterization is done by applying temperature cycles to the resonator and monitoring its resonance frequency and Q. For this purpose, the temperature is rapidly ramped down from 120 °C to −40 °C and then ramped up back to 120 °C. A temperature stabilization time of 1 h is considered between consecutive temperature changes prior to frequency and Q measurements. The measurement results for short-term hysteresis characterization after 22 cycles for resonance

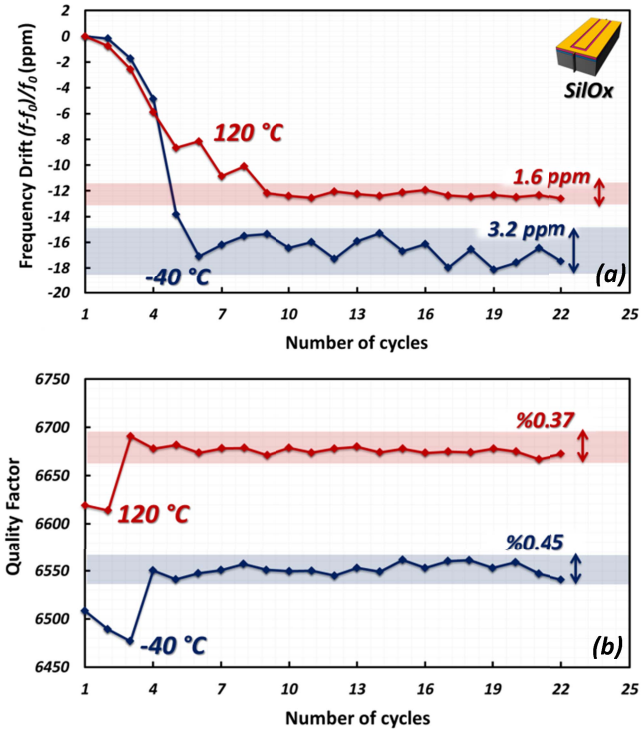

Fig. 14. Hysteresis characteristics of (a) resonance frequency and (b) Q of a SilOx resonator operating in WE_1 mode. The resonance frequency and Q of the device are measured after upward and downward halves of 22 consecutive wide temperature cycles between −40 °C and 120 °C, to evaluate performance stability under rapid temperature fluctuations. Each measurement takes place after holding for 1 h to reach thermal equilibrium.

frequency and Q are shown in Fig. 14. The stabilization behavior observed in the hysteresis characteristic of the resonance frequency is similar to the long-term stabilization at the elevated temperature (Fig. 13). The stabilization period is, however, considerably reduced in response to the rapid temperature cycling. This can be attributed to the higher efficiency of stress-release and thermo-mechanical processes in the resonator for the temperature cycling case. Overall frequency fluctuations of 1.6 and 3.2 ppm are measured, respectively, for 120 °C and −40 °C temperature points of the cycles in the stabilized period, while the Q remains stable after a slight increase over the stabilization period. The small frequency fluctuations can be attributed to the nonzero local TCF_1 of the measured device at two different temperatures and ±1 °C temperature accuracy of the chamber.

VI. Conclusion

This paper presented a new passive temperature compensation technique for silicon resonators. SiO_2 pillars were embedded by filling a matrix of uniformly distributed trenches etched in SCS to form SilOx composite homogenous platform. The distribution and in-plane dimensions of SiO_2 pillars in the matrix can be designed to provide nearly full temperature compensation for different/independent elastic moduli of interest. Analytical and numerical analyses were used to design for proper dimension and distribution of pillars to facilitate the excitation of desired resonance modes with compensated TCF_1. Resonators implemented in SilOx platforms did not show any degradation in Q and IL compared with their SCS counterparts. TCF_1 compensation of multiple in- and out-of-plane modes (i.e., $WE_{1,3}$, WS_1, LE_1, and TE_1 modes) of a rectangular SilOx microresonator was demonstrated. Overall frequency drifts as small as 83 ppm were measured over the temperature range of −40 °C to +80 °C. Such high-performance temperature-compensated devices were well suited for temperature-stable frequency reference applications, where the requirement of high Q and large power handling made thick silicon-based microresonators desirable.

References

[1] F. Ayazi, "MEMS for integrated timing and spectral processing," in *Proc. IEEE CICC*, Sep. 2009, pp. 65–72.

[2] R. Tabrizian, M. Rais-Zadeh, and F. Ayazi, "Effect of phonon interactions on limiting the f.Q product of micromechanical resonators," in *Proc. IEEE Int. Conf. Solid-State Sensors, Actuat. Microsyst.*, Jun. 2009, pp. 2131–2134.

[3] F. Ayazi, R. Tabrizian, and L. Sorenson, "Compensation, tuning and trimming of MEMS resonators," in *Proc. IEEE IFCS*, May 2012, pp. 1–7.

[4] K. Sundaresan, G. Ho, S. Pourkamali, and F. Ayazi, "Electronically temperature compensated silicon bulk acoustic resonator reference oscillators," *IEEE J. Solid-State Circuits*, vol. 42, no. 6, pp. 1425–1434, Jun. 2007.

[5] A. Tazzoli, M. Rinaldi, and G. Piazza, "Ovenized high frequency oscillators based on aluminum nitride contour mode MEMS resonators," in *Proc. IEEE IEDM*, Dec. 2011, pp. 481–484.

[6] J. C. Salvia, R. Melamud, S. A. Chandorkar, S. F. Lord, and T. W. Kenny, "Real-time temperature compensation of MEMS oscillators using an integrated micro-oven and a phase lock loop," *J. Microelectromech. Syst.*, vol. 19, no. 1, pp. 192–201, Feb. 2010.

[7] C. Chiang, A. B. Graham, E. J. Ng, C. H. Ahn, G. J. O'Brien, and T. W. Kenny, "A novel, high-resolution resonant thermometer used for temperature compensation of a cofabricated pressure sensor," in *Proc. Solid-State Sensors, Actuat., Microsyst. Workshop*, 2012, pp. 54–57.

[8] R. Melamud, S. A. Chandorkar, B. Kim, H. K. Lee, J. C. Salvia, G. Bahl, M. A. Hopcroft, and T. W. Kenny, "Temperature insensitive composite micromechanical resonators," *J. Microelectromech. Syst.*, vol. 18, no. 6, pp. 1409–1419, 2009.

[9] D. Grogg, H. C. Tekin, N. D. Ciressan-Badila, D. Tsamados, M. Mazza, and A. M. Ionescu, "Bulk lateral MEM resonator on thin SOI with high Q-factor," *IEEE/ASME J. Microelectromech. Syst.*, vol. 18, no. 2, pp. 466–479, Apr. 2009.

[10] A. K. Samarao, G. Casinovi, and F. Ayazi, "Passive TCF compensation in high Q silicon micromechanical resonators," in *Proc. IEEE 23rd Int. Conf. MEMS*, Jan. 2010, pp. 116–119.

[11] J. S. Wang and K. M. Lakin, "Low-temperature coefficient bulk acoustic wave composite resonators," *Appl. Phys. Lett.*, vol. 40, no. 4, pp. 308–310, Feb. 1982.

[12] W. Pan and F. Ayazi, "Thin-film piezoelectric-on-substrate resonators with Q enhancement and TCF reduction," in *Proc. IEEE Int. Conf. MEMS*, Jan. 2010, pp. 104–107.

[13] A. Hajjam, A. Rahafrooz, and S. Pourkamali, "Sub-100 ppm/°C temperature stability in thermally actuated high frequency silicon resonators via degenerate phosphorous doping and bias current optimization," in *Proc. IEEE IEDM*, Dec. 2010, pp. 170–173.

[14] M. Shahmohammadi, B. P. Harrington, J. Gonzales, and R. Abdolvand, "Temperature-compensated extensional-mode MEMS resonators on highly N-type doped silicon substrates," in *Proc. Solid-State Sensors, Actuat., Microsyst. Workshop*, 2012, pp. 371–374.

[15] A. K. Samarao and F. Ayazi, "Temperature compensation of silicon micromechanical resonators via degenerate doping," in *Proc. IEEE IEDM*, Dec. 2009, pp. 789–792.

[16] A. K. Samarao and F. Ayazi, "Intrinsic temperature compensation of highly resistive high-Q silicon microresonators via charge carrier depletion," in *Proc. IEEE IFCS*, Jun. 2010, pp. 334–339.

[17] A. Ballato and J. R. Vig, "Static and dynamic frequency-temperature behavior of singly and doubly rotated, oven-controlled quartz resonators," in *Proc. 32nd FCS*, 1978, pp. 180–188.

[18] R. Tabrizian, G. Casinovi, and F. Ayazi, "Temperature-stable high-Q AlN-on-silicon resonators with embedded array of oxide pillars," in *Proc. Solid-State Sensors, Actuat., Microsyst. Workshop*, 2010, pp. 100–101.
[19] R. Tabrizian, M. Pardo, and F. Ayazi, "A 27 MHz temperature compensated MEMS oscillator with sub-ppm instability," in *Proc. IEEE Int. Conf. MEMS*, Jan./Feb. 2012, pp. 23–26.
[20] G. Bahl, R. Melamud, B. Kim, S. Chandorkar, J. Salvia, M. A. Hopcroft, R. G. Hennessy, S. Yoneoka, C. M. Jha, G. Yama, D. Elata, R. N. Candler, R. T. Howe, and T. W. Kenny, "Observation of fixed and mobile charge in composite MEMS resonators," in *Proc. Solid-State Sensors, Actuat., Microsyst. Workshop*, 2008, pp. 102–105.
[21] C. Bourgeois, E. Steinsland, N. Blanc, and N. F. de Rooij, "Design of resonators for the determination of the temperature coefficients of elastic constants of monocrystalline silicon," in *Proc. IEEE Int. Freq. Control Symp.*, May 1997, pp. 791–799.
[22] J. R. Vig and T. R. Meeker, "The aging of bulk acoustic wave resonators, filters and oscillators," in *Proc. 45th Annu. Symp. Freq. Control*, 1991, pp. 77–101.
[23] J. A. Kusters and J. R. Vig, "Hysteresis in quartz resonators—A review," *IEEE Trans. Ultrason., Ferroelectr. Freq. Control*, vol. 38, no. 3, pp. 281–290, May 1991.

Roozbeh Tabrizian (S'06) is currently pursuing the Ph.D. degree with the Georgia Institute of Technology, Atlanta, GA, USA, with a focus on design, fabrication and characterization of piezoelctrically transduced micromechanical resonators for timing, signal processing and sensing applications.

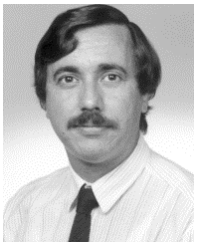

Giorgio Casinovi (M'89–SM'93) received the Ph.D. degree in electrical engineering from the University of California, Berkeley, CA, USA.

His current research interests include computer-aided design, modeling and simulation of electronic devices, circuits and microelectromechanical systems.

Farrokh Ayazi (S'96–M'00–SM'05–F'12) received the Ph.D. degree in electrical engineering from the University of Michigan, Ann Arbor, MI, USA, in 2000.

He is a Professor with the School of Electrical and Computer Engineering, GIT, Atlanta, GA, USA.